

Effect of spin-reorientation transition of cell boundary phases on the temperature dependence of magnetization and coercivity in Sm_2Co_{17} magnets

Si-Si Tu(涂思思), Lei Liu(刘雷), Bo Zhou(周波), Chuang-Hui Dong(董创辉), Li-Ming Ye(叶力铭), Ying-Li Sun(孙颖莉), Yong Ding(丁勇), A-Ru Yan(闫阿儒), and Xin-Biao Mao(毛信表)
Citation: Chin. Phys. B, 2023, 32 (**12**): 127501. DOI: 10.1088/1674-1056/acc80b
Journal homepage: http://cpb.iphy.ac.cn; http://iopscience.iop.org/cpb

What follows is a list of articles you may be interested in

Out-of-plane weak ferromagnetism at room temperaturein lattice-distortion non-collinear antiferromagnet of single-crystal Mn_3Sn

Bo-Xi Zhang(张博熙), Ping Song(宋平), Shan-Shan Deng(邓珊珊), Li Lou(娄理), and Sen Yao(姚森)
Chin. Phys. B, 2023, 32 (**8**): 087502. DOI: 10.1088/1674-1056/acca0b

Critical behavior in the itinerant ferromagnet $SmMn_2Ge_2$

Qingyi Hou(侯清漪), Meng Song(宋猛), Xitong Xu(许锡童), Yihao Wang(王宜豪), Chao Dong(董超), Yinfa Feng(冯寅发), Miao He(何苗), Yonglai Liu(刘永来), Liang Cao(曹亮), Junfeng Wang(王俊峰), Zhe Qu(屈哲), and Yimin Xiong(熊奕敏)
Chin. Phys. B, 2023, 32 (**8**): 087501. DOI: 10.1088/1674-1056/accb49

Electric-field control of perpendicular magnetic anisotropy by resistive switching via electrochemical metallization

Yuan Yuan(袁源), Lu-Jun Wei(魏陆军), Yu Lu(卢羽), Ruo-Bai Liu(刘若柏), Tian-Yu Liu(刘天宇), Jia-Rui Chen(陈家瑞), Biao You(游彪), Wei Zhang(张维), Di Wu(吴镝), and Jun Du(杜军)
Chin. Phys. B, 2023, 32 (**6**): 067505. DOI: 10.1088/1674-1056/acbde8

Crystal growth of $CeMn_{0.85}Sb_2$: Absence of magnetic order of Ce-sublattice

Yong Li(李勇), Shan-Shan Miao(苗杉杉), Hai Feng(冯海),Huai-Xin Yang(杨槐馨), and You-Guo Shi(石友国)
Chin. Phys. B, 2023, 32 (**6**): 067501. DOI: 10.1088/1674-1056/acc060

Magnetic triangular bubble lattices in bismuth-doped yttrium iron garnet

Tao Lin(蔺涛), Chengxiang Wang(王承祥), Zhiyong Qiu(邱志勇), Chao Chen(陈超), Tao Xing(邢弢), Lu Sun(孙璐), Jianhui Liang(梁建辉), Yizheng Wu(吴义政), Zhong Shi(时钟), and Na Lei(雷娜)
Chin. Phys. B, 2023, 32 (**2**): 027505. DOI: 10.1088/1674-1056/aca604

Effect of spin-reorientation transition of cell boundary phases on the temperature dependence of magnetization and coercivity in Sm_2Co_{17} magnets

Si-Si Tu(涂思思)[1,2], Lei Liu(刘雷)[2,†], Bo Zhou(周波)[2], Chuang-Hui Dong(董创辉)[2], Li-Ming Ye(叶力铭)[2], Ying-Li Sun(孙颖莉)[2], Yong Ding(丁勇)[2,‡], A-Ru Yan(闫阿儒)[2], and Xin-Biao Mao(毛信表)[1]

[1] *College of Chemical Engineering, Zhejiang University of Technology, Hangzhou* 310014, *China*

[2] *CISRI and NIMTE Joint Innovation Center for Rare Earth Permanent Magnets, CAS Key Laboratory of Magnetic Materials and Devices, Ningbo Institute of Materials Technology and Engineering, Chinese Academy of Sciences, Ningbo* 315201, *China*

(Received 21 February 2023; revised manuscript received 23 March 2023; accepted manuscript online 28 March 2023)

Four Sm_2Co_{17} magnets with spin-reorientation transition (SRT) of cell boundary phases (CBPs) are prepared by liquid-phase sintering. The temperature of the SRT of CBPs ($T_{SR}^{1:5}$) is regulated from 125 K to 195 K by adding 0 wt.%, 3 wt.%, 6 wt.% and 9 wt.% $Dy_{88}Cu_{12}$ alloy powder. The effect of SRT of Sm_2Co_{17} magnet CBPs on the temperature dependence of the magnetization (M–T) and coercivity (H–T) is systematically investigated. The temperature dependence of the magnetization is influenced by the SRT of CBPs. The M–T curves measured during the heating process are larger than those measured during the cooling process when $T < T_{SR}^{1:5}$. When $T = T_{SR}^{1:5}$ there is a bifurcation point. When $T > T_{SR}^{1:5}$ the M–T curves overlap and the M–T derivation curve shows that the magnetization of the magnet has low temperature dependence of magnetization above $T_{SR}^{1:5}$. With increasing $T_{SR}^{1:5}$, the initial temperature of the low temperature dependence of magnetization shifts towards a higher temperature. The coercivity temperature coefficient becomes positive as the SRT effect increases, and the temperature range of the positive coercivity temperature coefficient moves towards higher temperatures as $T_{SR}^{1:5}$ increases. This reveals that SRT of CBPs has little effect on the temperature dependence of magnetization above $T_{SR}^{1:5}$, while the temperature dependence of coercivity is optimized. The temperature range of magnetization and coercivity with low temperature dependence tends towards higher temperatures, which is conducive to the preparation of magnets with a low temperature coefficient at higher temperatures.

Keywords: spin-reorientation transformation, low-temperature coefficient, Sm_2Co_{17} magnets

PACS: 75.30.Gw, 68.60.Dv, 71.20.Eh, 75.50.Ww **DOI:** 10.1088/1674-1056/acc80b

1. Introduction

More accurate and light-weight low-cost magnetic and inertial measurement units are needed for the technological development of gyroscopes, accelerometers, sensors and traveling-wave tubes.[1,2] At the same time, more stringent requirements have been placed on the temperature stability of magnets. Sm_2Co_{17} magnets are the best candidates due to their high Curie temperature, good magnetic properties and excellent thermal stability. In general, the higher the coercivity of the magnet, the better the demagnetization resistance and the magnet's stability. However, recent studies[3,4] have shown that the irreversible and reversible flux losses of magnets are affected by their remanence temperature coefficient (α), and the magnetic drift caused by the change in the anti-demagnetization capacity of magnets is affected by the temperature coefficient of the coercivity (β). As a result, to meet high-precision measurement requirements, the α and β values of magnets should be low. Researchers[5–8] have attempted to achieve a low α value by replacing Sm with heavy rare earth (RE) elements (such as Gd, Er and Dy). Subsequently, researchers[9–12] discovered that a positive coercivity coefficient of temperature could be achieved by increasing the Sm content, reducing the content of Cu or performing an incomplete aging treatment (later referred to as the Cu-rich CB method). Since the Cu-rich CB method results in a positive coercive temperature coefficient by reducing the Cu content in the cell boundary phase (CBP), and the decrease in Cu content leads to a decrease in the coercivity of the magnet, this method contradicts existing knowledge regarding the fabrication of high-coercivity magnets.[13]

The $Sm_{1-x}Dy_x(Co_{0.695}Fe_{0.2}Cu_{0.08}Zr_{0.025})_{7.2}$ magnets with spin-reorientation transition (SRT) of the CBP (later referred to as the SRT-CB method) have reported a positive β value.[4] This result revealed that SRT of CBPs was responsible for abnormal coercivity. In contrast to the Cu-rich CB method, the SRT-CB method could result in high coercivity, and the positive temperature range could be varied by adding a RE (Nd, Pr, Dy, Tb).[4,14]

Paradoxically, because α and β are both related

†Corresponding author. E-mail: liulei@nimte.ac.cn

‡Corresponding author. E-mail: dingyong@nimte.ac.cn

© 2023 Chinese Physical Society and IOP Publishing Ltd

to the RE, it is unclear what effect SRT of CBPs has on the temperature dependence of the magnetization and coercivity of Sm_2Co_{17} magnets. In this study, $Sm_{0.6}Gd_{0.1}Dy_{0.3}(Co_{0.695}Fe_{0.2}Cu_{0.08}Zr_{0.025})_{7.8}$ alloy with SRT of CBPs and $Dy_{88}Cu_{12}$ alloy powder (Dy–Cu) are used as the base material and additive, respectively, to regulate $T_{SR}^{1:5}$ (the temperature of SRT of CBPs). Four Sm_2Co_{17} magnets with SRT of CBPs are prepared by doping 0 wt.%, 3 wt.%, 6 wt.% and 9 wt.% of Dy–Cu with liquid-phase sintering. The effects of SRT of CBPs on the temperature dependence of magnetization and coercivity are systematically studied.

2. Experimental details

A series of magnets with SRT of CBPs are prepared by liquid-phase sintering. The alloys $Sm_{0.6}Gd_{0.1}Dy_{0.3}(Co_{0.695}Fe_{0.2}Cu_{0.08}Zr_{0.025})_{7.8}$ and $Dy_{88}Cu_{12}$ were prepared by induction melting in an argon atmosphere. The alloys were then milled into powders with a particle size of approximately 3–5 μm. Additions of 0 wt.%, 3 wt.%, 6 wt.% and 9 wt.% of $Dy_{88}Cu_{12}$ as a base material were mixed and pressed under a magnetic field (3 T). Further compacting was followed by cold isostatic pressing to obtain a green compaction. After the green compaction was sintered at 1200–1220 °C for 2 h the solution was treated at 1160–1190 °C for 2 h and quenched in a furnace after being aged at 830 °C for 12 h.

The phase structure was examined by x-ray diffraction (XRD) with Cu $K\alpha$ radiation. The cellular structure and elemental distribution were observed with a transmission electron microscope (TEM) equipped for energy-dispersive x-ray spectroscopy. The SRTs were measured by a physical properties measurement system. The temperature stability was measured by a Quantum Design superconducting quantum interference device vibrating sample magnetometer. The magnetic properties were examined at the National Institute of Metrology (NIM-500C).

3. Results and discussion

The XRD patterns of the magnets doped with 0 wt.%, 3 wt.%, 6 wt.% and 9 wt.% Dy–Cu are shown in Fig. 1. According to the PDF card, all samples consist mainly of two phases: a Th_2Zn_{17}-type rhombohedral phase (2:17R, i.e., cell phase) and a $CaCu_5$-type hexagonal phase (1:5H, i.e., CBP). With increasing Dy–Cu doping, the diffraction peak intensity of the magnets at approximately 42.7° tends to increase; this could be the increase in the 1:5H phase content of the magnets.

The cellular microstructure and the Dy and Cu element distributions were observed by TEM. The results for the magnets doped with 0 wt.%, 3 wt.% and 9 wt.% Dy–Cu are shown in Figs. 2(a)–2(c). As shown in Fig. 2(a), the cell structure of the magnet without Dy–Cu doping is nonuniform, and the CBP is discontinuous. The statistical results show that the average size of the cell structure is approximately 100 nm. The line scanning results show that the CBP is Cu-rich and Dy-poor compared with the cell interiors. High-resolution electron microscope analysis shows that the thickness of the CBP is approximately 10 nm. As shown in Fig. 2(b), the cellular structure of the 3 wt.% Dy–Cu doped magnet appears to be more uniform and complete than that of the magnet without Dy–Cu doping. The statistical calculation results show that the average size of the cell structure is approximately 80 nm. The distribution of Dy in the cellular structure seems more uniform, and the thickness of the CBP increases to approximately 15 nm. As shown in Fig. 2(c), the size of the cellular structure of the magnet doped with 9 wt.% Dy–Cu is small. As Dy stabilizes the 2:17H phase and prolongs the aging time,[15] some areas are not as large as they would normally be. The statistical results show that the average size of the cell structure is approximately 50 nm, and the Dy content in the CBP is higher than that in the cell interiors. The thickness of the CBP is approximately 23 nm. The results of morphological observation, statistical calculation and high-resolution electron microscopy analysis show that the number, thickness and volume fraction of the 1:5H CBP increase with the ratio of Dy–Cu doping. This is consistent with the results of XRD analysis. Moreover, the addition of Dy–Cu is conducive to the segregation of Dy at the cell boundary, and (Sm, Dy)(Co, Cu)$_5$ compounds with spin reorientation are formed.[16–18]

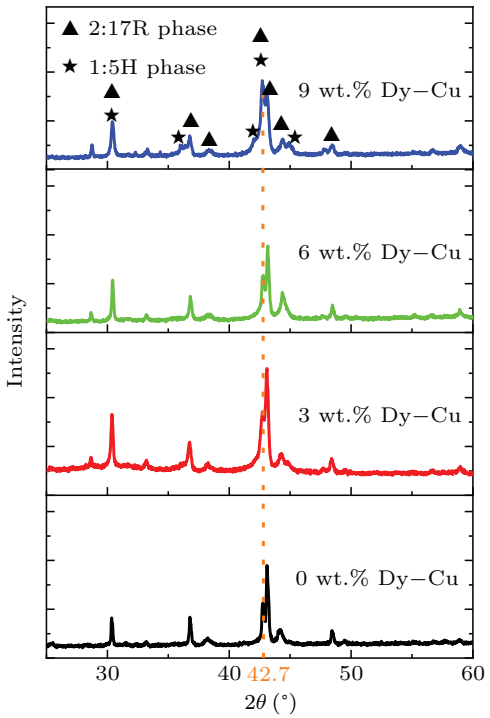


Fig. 1. XRD patterns of the magnets doped with 0 wt.%, 3 wt.%, 6 wt.% and 9 wt.% Dy–Cu.

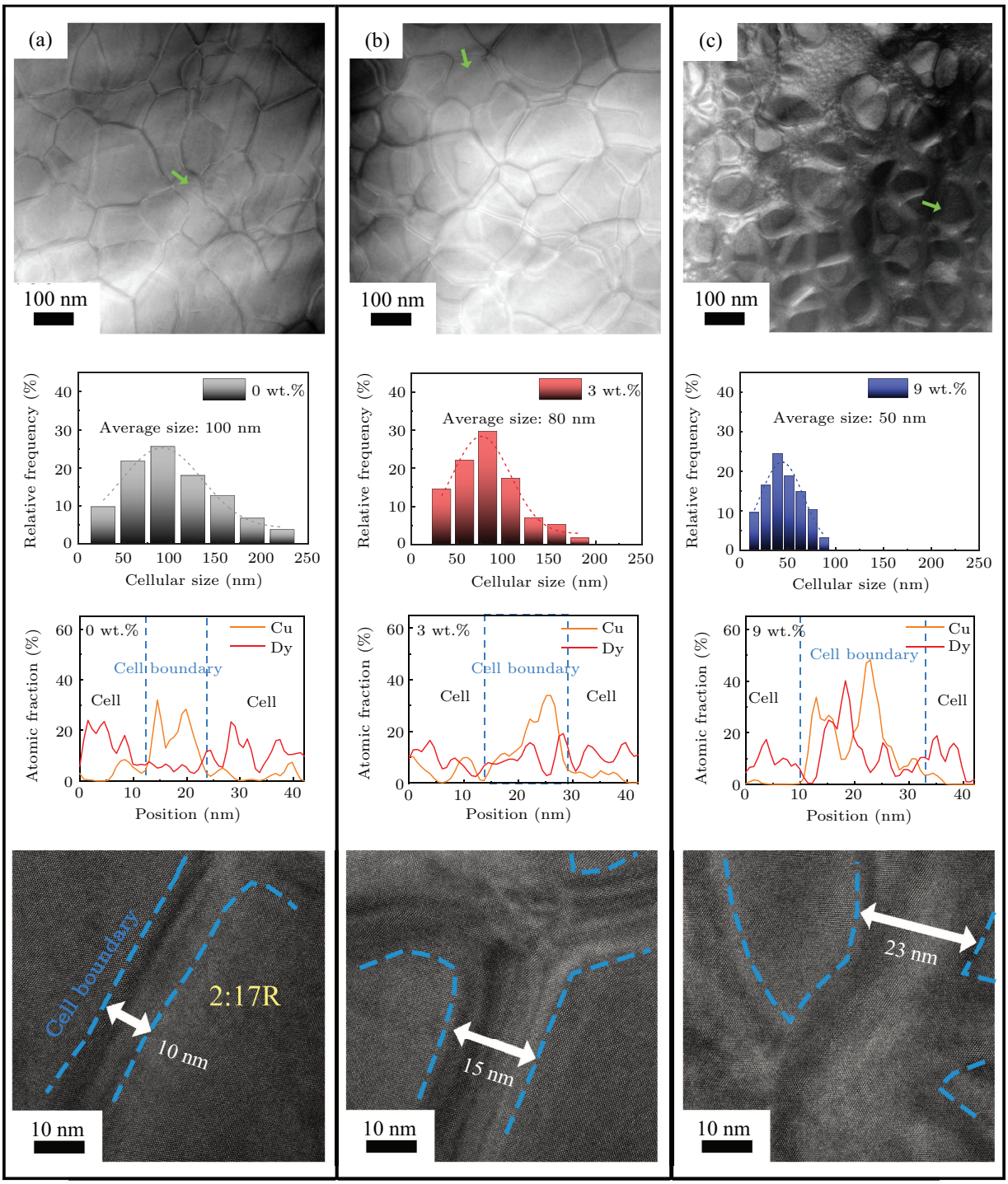


Fig. 2. TEM analysis of magnets doped with (a) 0 wt.%, (b) 3 wt.% and (c) 9 wt.% Dy–Cu.

As shown in Fig. 3, the AC susceptibility was characterized to determine the $T_{SR}^{1:5}$ of each sample. The parameters chosen for our measurements were as follows: AC field of 5 Oe, heating rate of 5 K·min^{-1} and a frequency of 1000 Hz. There is a peak in the test results for each sample. According to Kronmüller and Goll,[13] the peak corresponds to $T_{SR}^{1:5}$. The $T_{SR}^{1:5}$ values for the magnets doped with 0 wt.%, 3 wt.%, 6 wt.% and 9 wt.% Dy–Cu are 125 K, 145 K, 170 K and 195 K, respectively. As the amount of Dy–Cu doping increases, the content of (Sm, Dy)(Co, Cu)$_5$ in the CBPs increases and $T_{SR}^{1:5}$ increases, indicating that the effect of SRT of CBPs is enhanced. At this point, it is confirmed that four Sm_2Co_{17} magnets with SRT of CBPs were prepared.

To understand the effect of SRT of CBPs on the temperature dependence of the magnetization, thermal magnetic analysis was performed on these magnets. The sample was first magnetized to saturation with a 5 T magnetic field at 5 K and then measured in the temperature range of 5–400 K in a field of 50 Oe. Next, a 5 T magnetic field was applied again to the magnets at 400 K. The sample was measured in the temper-

ature range of 400–5 K in a field of 50 Oe. All the cooling and heating rates were 10 K·min^{-1}. Figure 4(a) shows the result for the magnetization curves measured during the cooling and heating processes. It is interesting to note that the magnetization curves measured during the heating process exhibit sharp decreases due to the influence of SRT on the behavior of the CBP and the temperature dependence of the intrinsic spin magnetic moment of the magnet alloy. The M–T curve measured during the heating process is larger than that measured during the cooling process when the temperature is below the peak temperature. There are two reasons for this: on the one hand the diamagnetism of the magnet is weakened by the effect of SRT on the behavior of the CBPs, on the other hand the spin magnetic moment of Dy increases at low temperatures, causing the overall magnetic moment of the magnet to decrease. After the sharp decrease, a bifurcation point appears. For the results of the AC susceptibility test, $T_{SR}^{1:5}$ is marked with a star. The bifurcation point is discovered to be close to $T_{SR}^{1:5}$. After the bifurcation point, the M–T curves overlap. To further analyze the coinciding part of the magnetization curves, we derived the magnetization from the temperature. The result is shown in Fig. 4(b). The absolute value of the derivative of less than 0.001 was taken as the limit, and the dotted lines are used to circle the range. The starting points of the overlapping temperature ranges are 155 K, 185 K, 220 K and 245 K with doping amounts of 0 wt.%, 3 wt.%, 6 wt.% and 9 wt.%, respectively. This indicates that the series of magnets have a low temperature dependence of magnetization above $T_{SR}^{1:5}$, and as $T_{SR}^{1:5}$ increases, the initial temperature of the low temperature dependence of the magnetization moves to a higher temperature.

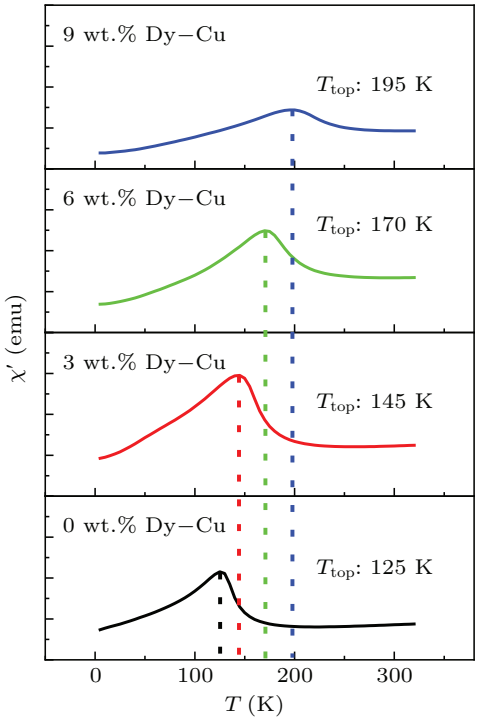


Fig. 3. Temperature dependence of the real part of the AC susceptibility of the magnets doped with 0 wt.%, 3 wt.%, 6 wt.% and 9 wt.% Dy–Cu.

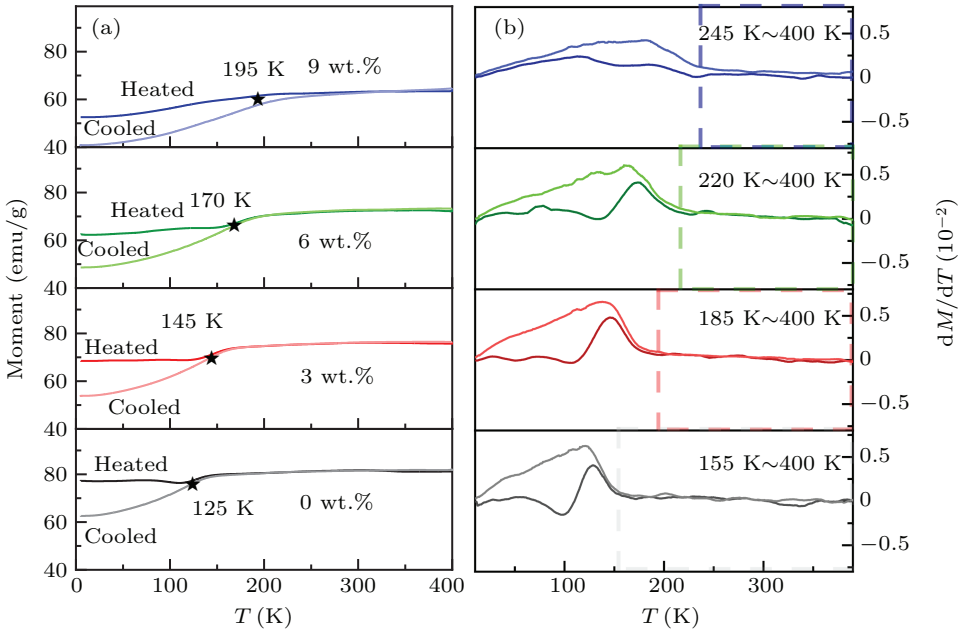


Fig. 4. (a) Temperature dependence of the magnetization (M–T curves) for the magnets doped with 0 wt.%, 3 wt.%, 6 wt.% and 9 wt.% Dy–Cu. (b) Temperature dependence of $\mathrm{d}M/\mathrm{d}T$ for the magnets doped with 0 wt.%, 3 wt.%, 6 wt.% and 9 wt.% Dy–Cu.

Both the temperature dependence of the magnetization and the temperature dependence of the coercivity are influenced by SRT of CBPs. For example, the temperature dependence of the coercivity H_{cj} of these magnets at 5–400 K is shown in Fig. 5. Without Dy–Cu doping, H_{cj} decreases monotonically with increasing temperature. A positive coercivity temperature coefficient is observed with increase in the amount of Dy–Cu doping. When the amount of Dy–Cu doping

is 3 wt.%, the magnetic crystal anisotropy of the 2:17R phase decreases monotonically with increasing temperature, while the magnetic crystal anisotropy of the 1:5H phase increases first and then decreases with the spin-reorientation phase transition. The synergistic effect of 2:17R and 1:5H results in an inflection point of the H–T curve at approximately 150 K. When the sample is doped with 6 wt.% Dy–Cu, the corresponding temperatures of the minimum H_{cj} (3.62 kOe) and maximum H_{cj} (8.20 kOe) are 150 K and 350 K, respectively. The sample doped with 9 wt.% Dy–Cu has a minimum H_{cj} (1.63 kOe) that corresponds to a temperature of 250 K. The extreme point of coercivity tends to move to high temperatures with increasing $T_{SR}^{1:5}$. The temperature dependence of the coercivity near the extreme point is relatively stable, and the temperature range near the maximum H_{cj} performs better than that near the minimum H_{cj} for obtaining a higher coercivity and a wide range of temperature stability. A wide range of temperature stability is also called a positive coercivity temperature coefficient range. This means that the positive coercivity temperature coefficient temperature range of the magnet moves towards higher temperatures with increasing $T_{SR}^{1:5}$.

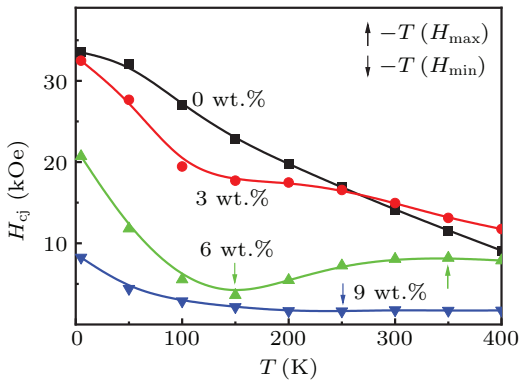


Fig. 5. Temperature dependence of the coercivity of magnets doped with 0 wt.%, 3 wt.%, 6 wt.% and 9 wt.% Dy–Cu.

It is found that SRT of CBPs can optimize the coercivity temperature coefficient with little effect on the temperature dependence of magnetization. Moreover, the temperature range of low-temperature-dependent magnetization and coercivity tends to move towards higher temperatures, which is conducive to the preparation of magnets with a low temperature coefficient at higher temperatures. The magnet doped with 6 wt.% Dy–Cu exhibits ideal temperature stability near room temperature. As a result, the demagnetization curves of the magnets were precisely compared in the range from room temperature (RT) to 100 °C with a NIM 500C magnetic measuring device every 20 °C. As shown in Fig. 6(a), a low point is observed for the magnet without Dy–Cu doping, for which the magnetic properties are $B_r = 8.71$ kG, $H_{cj} = 16.37$ kOe, $(BH)_{max} = 17.61$ MGOe, $\alpha = 0.01$ %·°C^{-1} and $\beta = -0.32$ %·°C^{-1}. Low α and β values for the magnet with 6 wt.% Dy–Cu doping are shown in Fig. 6(b), at which point the magnetic properties are $B_r = 7.80$ kG, $H_{cj} = 8.03$ kOe, $(BH)_{max} = 13.45$ MGOe, $\alpha = 0.01$ %·°C^{-1} and $\beta = -0.03$ %·°C^{-1}. Both their $\alpha_{(RT-100\,°C)}$ values are similar, while the $\beta_{(RT-100\,°C)}$ values decrease from -0.32 %·°C^{-1} to 0.03 %·°C^{-1}.

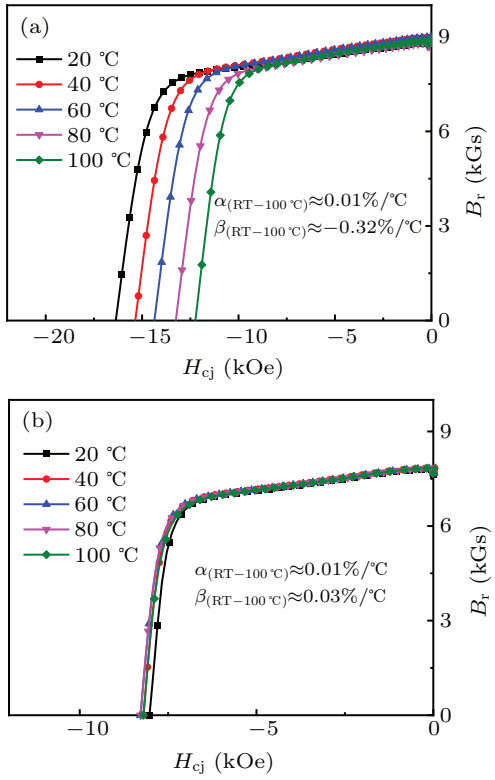


Fig. 6. Demagnetization curves of the magnets with different amounts of Dy–Cu doping of (a) 0 wt.% and (b) 6 wt.%. in the range from RT to 100 °C.

4. Conclusion

A series of samples with SRT in CBPs of Sm_2Co_{17} magnets were designed and prepared by doping with 0 wt.%, 3 wt.%, 6 wt.% and 9 wt.% of $Dy_{88}Cu_{12}$ alloy powder. $T_{SR}^{1:5}$ is regulated from 125 K to 195 K. The effect of SRT in CBPs of Sm_2Co_{17} magnets on the temperature dependence of the magnetization and coercivity was systematically investigated. The main findings are as follows:

(1) A variation in the temperature dependence of the magnetization is found to be influenced by SRT of CBPs. The M–T curves measured during the heating process are larger than those measured during the cooling process when $T < T_{SR}^{1:5}$. There is a bifurcation point when $T = T_{SR}^{1:5}$. When $T > T_{SR}^{1:5}$, the M–T curves overlap and the M–T derivation curve shows that the magnet has a low temperature dependence of magnetization above $T_{SR}^{1:5}$. With increasing $T_{SR}^{1:5}$, the initial temperature for low temperature dependence of magnetization shifts to a higher temperature.

(2) The coercivity temperature coefficient becomes positive as the effect of SRT of CPBs increases. With increasing $T_{SR}^{1:5}$, the temperature range shifts towards higher temperatures. This is beneficial for regulating the temperature range of Sm_2Co_{17} magnets with low β values.

(3) SRT of CBPs has little effect on the low temperature dependence of magnetization above $T_{SR}^{1:5}$, while the temperature coefficient of coercivity is optimized. The temperature range of magnetization and coercivity with low temperature dependence tends to move towards higher temperatures, which is conducive to the preparation of magnets with a low temperature coefficient at higher temperatures.

Acknowledgements

Project supported by the National Key R&D Program of China (Grant Nos. 2021YFB3803003 and 2021YFB3503101), Youth Innovation Promotion Association of CAS (Grant No. 2023311), Major Project of 'Science and Technology Innovation 2025' in Ningbo (Grant No. 2020Z044), and Zhejiang Provincial Key Research and Development Program (Grant No. 2021C01172).

References

[1] Bergamini E, Ligorio G, Summa A, Vannozzi G, Cappozzo A and Sabatini A 2014 *Sensors* **14** 18625
[2] Nazarahari M and Rouhani H 2021 *Inf. Fusion* **68** 67
[3] Rong C, Zhang H, Shen B and Liu J P 2006 *Appl. Phys. Lett.* **88** 042504
[4] Liu L, Liu Z, Zhang X, Zhang C Y, Li T Y, Lee D and Yan A R 2019 *J. Magn. Magn. Mater.* **473** 376
[5] Li D, Xu E, Liu J and Du Y 1980 *IEEE Trans. Magn.* **16** 988
[6] Gjoka M, Panagiotopoulos I, Niarchos D, Matthias T and Fidler J 2004 *J. Alloys Compd.* **367** 262
[7] Chen C H, Gong W, Walmer M H, Liu S and Kuhl G E 2002 *J. Appl. Phys.* **91** 8483
[8] Ji J G, Yang J B, Mao W H, Yang Y C, Li W and Yu X J 1998 *Solid State Commun.* **108** 667
[9] Liu J F, Chui T, Dimitrov D and Hadjipanayis G C 1998 *Appl. Phys. Lett.* **73** 3007
[10] Gutfleisch O, Müller K H, Khlopkov K, Wolf M, Yan A, Schäfer R, Gemming T and Schultz L 2006 *Acta Mater.* **54** 997
[11] Yan A, Bollero A, Müller K H and Gutfleisch O 2002 *Appl. Phys. Lett.* **80** 1243
[12] Liu S, Yang J, Doyle G, Potts G and Kuhl G E 2000 *J. Appl. Phys.* **87** 6728
[13] Kronmüller H and Goll D 2006 *J. Iron Steel Res.* **13** 39
[14] Zhao T S, Jin H M, Guo G H, Han X F and Chen H 1991 *Phys. Rev. B* **43** 8593
[15] Shen J, Qian P and Chen N X J 2004 *Phys. Chem. Solids* **65** 1307
[16] Banerjee D, Bahadur D, Suresh K G and Nigam A K 2006 *Physica B* **378** 1091
[17] Liu L, Pan DL, Liu Z, Zhang H W, Li M, Chen R J, Liu X M, Yan A R, Lee D and Li W 2015 *J. Magn. Magn. Mater.* **374** 634
[18] Liu Z, Liu L, Chen R J, Sun Y L, Lee D and Yan A R 2013 *IEEE Trans. Magn.* **49** 5599